Masood Mehrabian* and Parinaz Abdollahian

Improving Charge Transport in PbS Quantum Dot to Al:ZnO Layer by Changing the Size of Quantum Dots in Hybrid Solar Cells

DOI 10.1515/zna-2016-0204
Received May 21, 2016; accepted September 21, 2016; previously published online October 15, 2016

Abstract: PbS Quantum dots and P3HT are promising materials for photovoltaic applications due to their absorption in the NIR and visible region, respectively. Our previous experimental work showed that doping Al to ZnO lattice (Al:ZnO) could efficiently improve the cell performance. In this article, hybrid solar cells containing of two active areas with ITO/Al:ZnO/PbS QDs/P3HT&PCBM/Ag structure were fabricated and the effect of PbS QD size on photovoltaic properties was investigated. Optimised solar cell showed maximum power conversion efficiency of 2.45 % with short-circuit current of 9.36 mA/cm^2 and open-circuit voltage of 0.59 V under 1 sun illumination (AM1.5).

Keywords: Al-doped ZnO; Charge Transport; PbS Quantum Dots; Solar Cell.

1 Introduction

Quantum dots (QDs) are small nanoparticles of semiconductors and are referred to as artificial atoms due to their discrete electronic energy levels. However, the spacing between these electronic energy levels can be tuned by changing the size of the nanoparticle [1].

Bulk Lead sulfide (PbS) is an inorganic IV–VI semiconductor with a narrow band gap of 0.42 eV and exciton Bohr radius of 18 nm [2]. Presently, researchers have strongly focused on QD-sensitised solar cells (QDSSCs).

Using of narrow band gap semiconductor materials such as PbSQDs as light-absorbing layer in photovoltaic devices offers an efficient way to harvest the solar light in both the visible and infrared regions.

***Corresponding author: Masood Mehrabian,** Faculty of Basic Science, University of Maragheh, PO Box 55181-83111, Maragheh, Iran, E-mail: masood.mehrabian@yahoo.com; masood.mehrabian@maragheh.ac.ir
Parinaz Abdollahian: Department of Materials Engineering, Faculty of Engineering, University of Maragheh, PO Box 55181-83111, Maragheh, Iran

Zinc oxide (ZnO) is an excellent semiconductor material for the solar cell due to its high electron mobility, direct and wide band gap (3.37 eV), in the near-UV spectral region, large free-exciton binding energy (60 meV), and high chemical and thermal stability.

The electrical and optical properties of ZnO could be changed by chemical doping using materials such as aluminum. Al-doped zinc oxide (Al:ZnO or AZO) film is a candidate which could be used as transparent electrode in PV devices. AZO has many advantages such as high conductivity and optical transmittance in visible region, low cost and nontoxicity [3].

In our previous work, Aluminum-doped zinc oxide (AZO) thin films with various concentrations of Al were prepared and the photovoltaic properties of solar cells with ITO/AZO/P3HT&PCBM/Ag structure were investigated. Experimental results showed that maximum power conversion efficiency of 2.15 % could be obtained for device containing 20 wt% Al, while power conversion efficiency for undoped ZnO films was 1.5 % [4].

In this article, AZO films (containing of 20 wt% Al) were deposited on prepatterned indium-doped tin oxide (ITO) glass substrates by the sol–gel (spin coating) technique to overcome charge-transport limitations associated with organic materials. To prepare photo-electrodes, PbSQDs were directly grown on the AZO layers by the successive ionic layer absorption and reaction (SILAR) technique. We demonstrated that the number of SILAR cycles has an active effect on photovoltaic performance of the device.

2 Experiments

AZO precursor solution was prepared using zinc acetate dehydrate ($Zn(CH_3COO)_2{\cdot}2H_2O$), diethanolamine (DEA, $C_4H_{11}NO_2$), and aluminium nitrate ($Al(NO_3)_3{\cdot}9H_2O$) dissolved in ethanol. The prepared precursor solution was stirred at 70 °C for 90 min to yield a clear and homogenous solution. Al-doped ZnO nanoparticle thin films were prepared by sol–gel (spin-coating) method with spinning speed of 4500 rpm for 30 s. The molar ration of Al/Zn

was kept at 20 %. Then, films were preheated at 150 °C for 10 min and finally annealed at 500 °C for 2 h in air ambient. The final thickness of films was about 70 nm.

To fabricate photo-electrodes, obtained AZO layers were coated by PbS QDs using spin-assisted SILAR technique.

To do this, lead nitrate Pb $(NO_3)_2$ and sodium sulfide (Na_2S) were used as cationic and anionic solutions (Pb^{2+} and S^{2-} sources), respectively.

Appropriate amount of cationic solution dropped on the AZO layer and spin coated at 4500 rpm for 30 s. Then the same amount of anionic solution dropped on (cation-absorbed) substrate and spin coated at 4500 rpm for 30 s. These two-step procedures form one SILAR cycle (n). The coating process was repeated n times, herein referred to as PbS (n).

The PbS film became darker by increasing the number of SILAR cycles. The size and morphology of fabricated nanoparticles were varied by increasing the n. As a result, the band-gap energy was varied as it strongly depends on the size of the QDs.

To fabricate the PbS, QD-sensitised solar cell (PbS QDSSC) with ITO/AZO/PbS/P3HT&PCBM/Ag structure, a solution mixture of poly(3-hexylthiophene) (P3HT):phenyl C_{61} butyric acid methyl ester ($PC_{61}BM$) dissolved in the 1,2-dichlorobenzene (ODCB) was spin coated on photo-electrode at spin speed of 600 rpm for 50 s. Then, a thin layer of silver (100 nm) was sputtered over the device that will act as back contact. Now the device is ready for testing.

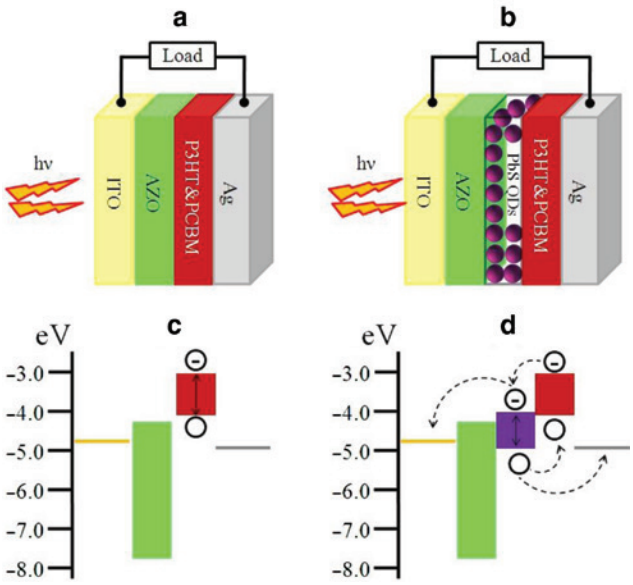

Figure 1: Schematic diagram of the (a) reference cell, (b) PbS QDSSC, energetic diagram of the (c) reference cell, (d) PbS QDSSC, and charge transfer of electrons towards ITO and holes towards Ag.

3 Results and Discussion

The schematic diagram of fabricated device with and without PbS QD layer, as well as the corresponding energy level diagramis shown in Figure 1 [5, 6].

The cell with ITO/AZO/P3HT&PCBM/Ag structure is referred as the reference cell (Figure 1a).

In the reference cell (Figure 1c), P3HT is the active layer that absorbs the visible region of incident light (up to 650 nm). However, in PbS QDSSC (Figure 1d), there are two active layers (P3HT and PbS) which cooperate in incident light absorbing. In the presence of near infrared (NIR) light, the PbS QD layer absorbs the light and generates excitons (electron–hole pairs).

To generate photo-current, these excitons have to be dissociated as electrons and holes. Then, these generated electrons (photoelectrons) should be transferred firstly towards the conduction band (CB) of the AZO layer, while the holes are moved to Ag contact and collected at this electrode (dashed lines in Figure 1d).

The surface morphology of AZO thin film and fabricated PbS QDs with different number of SILAR cycles were analysed by a Hitachi S-4160 FE scanning electron microscopy (FE-SEM) and are shown in Figure 2.

The structural characterisation of fabricated PbS QDs was measured by Philips (X'Pert Pro MPD) X-ray diffractometer with (40 kV and 40 mA) CuKα radiations ($\alpha = 1.5404$ Å) in 2θ range from 25° to 70° and is shown in Figure 2b. The diffraction peaks occur at 30°, 35°, 50°, 60°, and 63°, which are related with (111), (200), (220), (311), and (222) crystalline planes of cubic phase of PbS, respectively [7, 8].

It could be seen from Figure 2a, c–e that AZO thin layer, PbS(1), PbS(2), and PbS(3) have smooth, uniform, and flat surfaces. However, inPbS(4), PbS(5), and PbS(6), QDs are stacked on each other, making rough and nonuniform surfaces, as shown in Figure 2f–h. The thickness of AZO layer, PbS(1), PbS(5), and PbS(6) was 70 nm, 27 nm, 73 nm, and 85 nm, respectively.

It is observed that for $n > 3$, the PbS nano-particles agglomerate and the QD layer becomes darker; therefore, the incident light cannot reach to P3HT. As a result, the cell performance will decrease by (n).

The optical properties of PbS QDs with different number of SILAR cycles were characterised by performing transmission measurements using Perkin Elmer UV–Vis spectrophotometer.

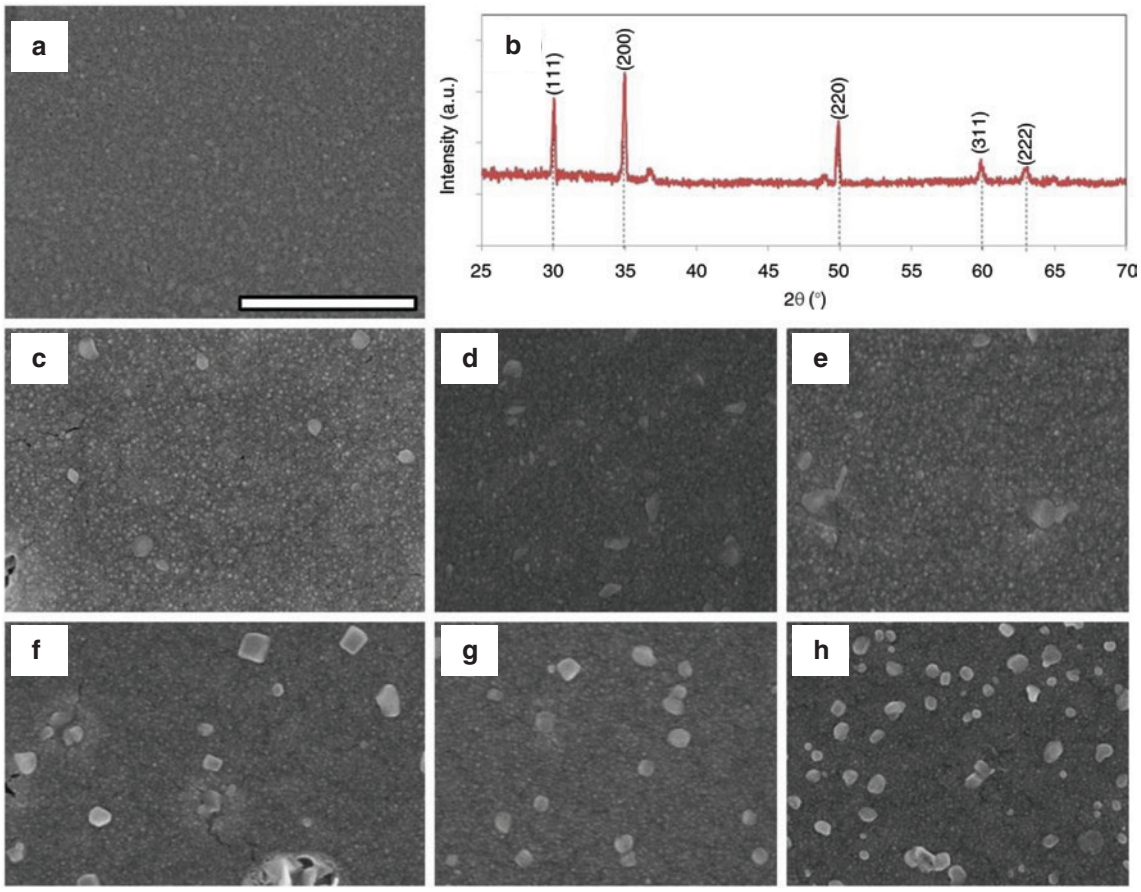

Figure 2: (a) SEM image of AZO thin film, (b) X-ray diffraction pattern of PbS QD layer, SEM images of (c) PbS(1), (d) PbS(2), (e) PbS(3), (f) PbS(4), (g) PbS(5), and (h) PbS(6) QDs deposited on glass substrates. Scale bar: 1 μm.

The transmittance spectra of fabricated PbS QD layers is depicted in Figure 3. It is clear that all films have high transparency in the visible range (400–700 nm). The transmittance of PbS QD layers in the wavelength range 400–700 nm is found to be 90, 86, 85, 94, 82, and 80 % for PbS(1), PbS(2), PbS(3), PbS(4), PbS(5), and Pbs(6), respectively. That is, there is a decrease in transparency as the number of SILAR cycles increases.

The band gap energy (E_g) values of PbS(n) calculated by plotting $(\alpha \text{th}\vartheta)^2$ versus (hϑ) as shown in the insets of Figure 3. The band gap energy for PbS QDs was found to vary in the range 1.6–0.95 eV, depending on the number of SILAR cycles (n). This reduction of band-gap energy corresponds to a red-shift (red-shift), which suggests a growth in PbS QD size with increasing (n) in the quantum size regime (quantum confinement effect) [9–11].

To determine the size of the PbSQDs, we used the Brus equation [12], as shown in (1):

$$E_g^{QD} - E_g^{Bulk} = \frac{h^2}{8r^2}\left(\frac{1}{m_e} + \frac{1}{m_h}\right)$$

where E_g^{QD}, E_g^{Bulk}, m_e, and m_h are the band gap of the QD, band gap of bulk material (0.42 eV), effective mass of electron (0.08 m_0), and hole (0.075 m_0), respectively.

The m_o is the free electron rest mass. The particle sizes of PbS QDs as well as their corresponding E_g are listed in Table 1.

The photovoltaic properties of solar cells with ITO/AZO/PbS(n)/P3HT&PCBM/Ag structure were investigated at room temperature with a Keithley 2400 source meter under AM 1.5G illumination at 100 mW/cm^2 supplied from a 150-W Oriel solar simulator. The current density–voltage (J–V) curves are shown in Figure 4.

The effect of QD size on the cell performance of PbS QDSSCs was analysed and the detailed values of cell parameters including short circuit current density (J_{sc}), open circuit voltage (V_{oc}), fill factor (FF), and power conversion efficiency (η) are listed in Table 2.

The power conversion efficiency values are 2.15 %, 2.38 %, 2.45 %, 2.40 %, 2.31 %, 2.26 %, and 1.65 %, respectively, corresponding to different devices of reference cell, electrodes containing of PbS(1), PbS(2), PbS(3), PbS(4), PbS(5), and PbS(6).

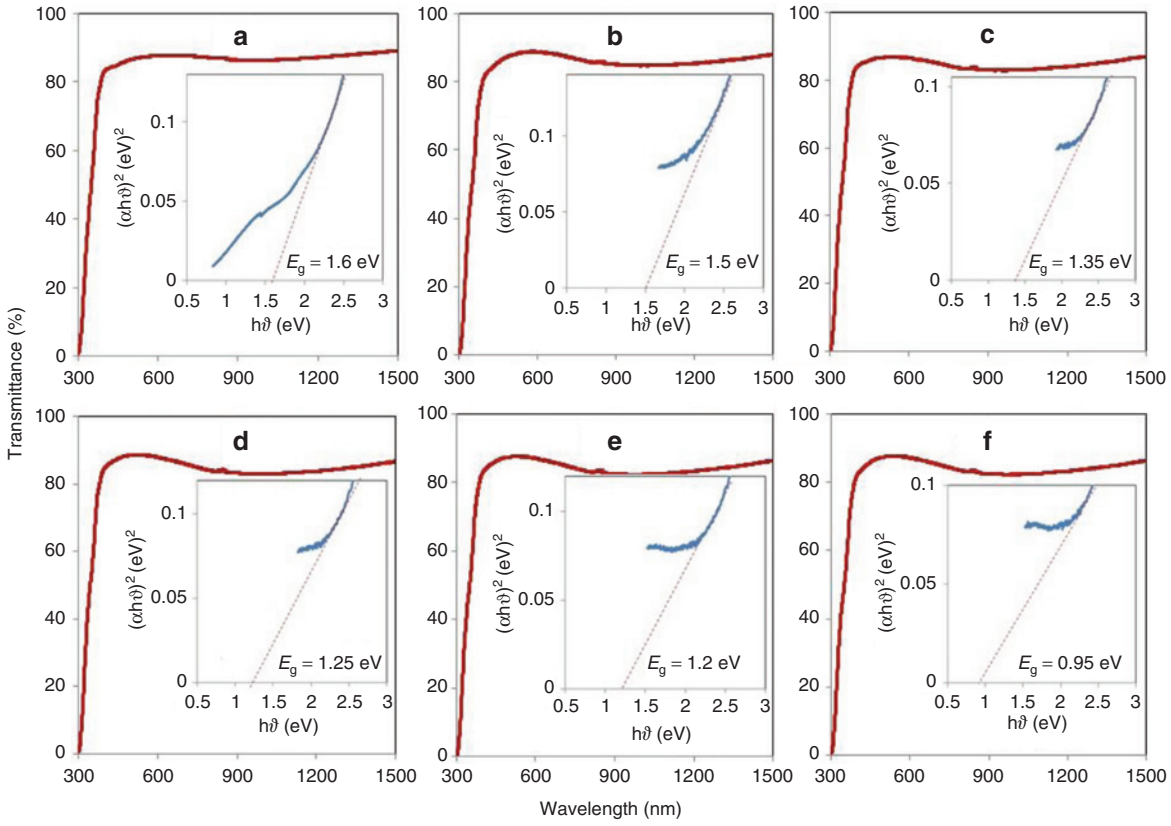

Figure 3: Optical transmittance of (a) PbS(1), (b) PbS(2), (c) PbS(3), (d) PbS(4), (e) PbS(5), and (f) PbS(6) quantum dots. Insets show the plot of $(\alpha h\vartheta)^2$ versus $(h\vartheta)$ for samples.

Table 1: Optical band gap and particle size of the PbS QDs with different number of cycles (n).

Sample	E_g (eV)	Particle size (nm)
PbS(1)	1.60	5.7
PbS(2)	1.50	6.1
PbS(3)	1.35	6.6
PbS(4)	1.25	7.2
PbS(5)	1.20	7.6
PbS(6)	0.95	8.2

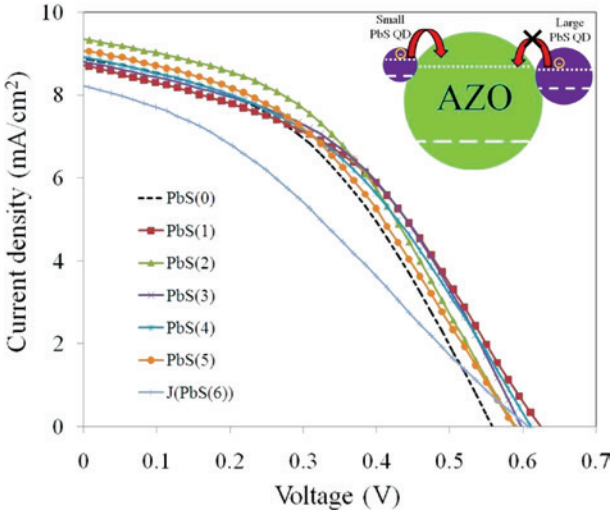

Figure 4: J–V curves of solar cells with ITO/AZO/PbS(n)/P3HT&PCBM/Ag structure. The inset shows the schematic of the relative alignment of the conduction and valence bands of AZO and PbS QDs (dotted and dashed lines, respectively) depending on the QD size.

The maximum power conversion efficiency of 2.45% was obtained for PbS(2), indicating that $n=2$ is the optimum number of cycles for a device with ITO/AZO/PbS(n)/P3HT&PCBM/Ag structure.

In devices containing of PbS(1) and PbS(2), the wider band gap shifting the CB of PbS to higher energies than CB of AZO, allowing photo-electron injection from PbS (with small size) into AZO.

According to quantum confinement effect, increasing the number of SILAR cycles from 2 to 6 leads to increase in QD size from 6.1 nm to 8.2 nm. The large PbS QDs ($n>2$) cannot inject photo-electrons into AZO CB as their CB is lower than the CB of AZO, as shown schematically in the inset of Figure 4.

Table 2: Photovoltaic performance of PbS QD-sensitised solar cells with different number of SILAR cycles (n) at 100 mw/cm^2 and AM 1.5 simulated solar light.

Electrode	V_{oc} (V)	J_{sc} (mA/cm^2)	FF (%)	Efficiency (%)
AZO + PbS(0)	0.56	8.88	43.03	2.15
AZO + PbS(1)	0.63	8.82	42.57	2.38
AZO + PbS(2)	0.59	9.36	43.28	2.45
AZO + PbS(3)	0.60	8.80	45.25	2.40
AZO + PbS(4)	0.61	8.91	42.00	2.31
AZO + PbS(5)	0.59	9.10	41.41	2.26
AZO + PbS(6)	0.61	8.22	32.32	1.65

As the size of PbS QD increases, the energetic distance between both CBs decreases, reducing the injection driving force and consequently the photocurrent from 9.36 mA/cm^2 to 8.80 mA/cm^2. This indicates that in solar cells with ITO/AZO/PbS(n)/P3HT&PCBM/Ag structure, PbS QDs with the particle size of 6.1 nm could be served as efficient active layer which effectively injects photoelectrons to AZO layer.

The size of QD has another effect on the cell performance, which could be explained as follow. In large QDs, the valence band (VB) of QD is getting closed to CB of AZO. Therefore, the electrons in the CB of AZO, which come from CB of PbS QD, will be recombined with holes in the VB of PbS instead of transferring to ITO and forming the photocurrent.

4 Conclusion

We could successfully fabricate solar cells with ITO/AZO/PbS(n) QD/P3HT&PCBM/Ag structure. PbS QD layer was deposited by spin-assisted SILAR technique with various numbersof cycles (n). In this device, both PbS and P3HT layers absorb the NIR and visible light, respectively. For two SILAR deposition cycles (PbS (2)), the solar cell with the highest energy conversion efficiency of 2.45 % was obtained. Experimental results showed that increasing the size of PbS QD from 6.1 nm to 8.2 nm leads to decrease the cell performance as a result of poor electron injection from CB of PbS to that of AZO. The effect of particle size on photovoltaic properties was investigated from the J–V characteristics.

References

[1] Z. Tachan, I. Hod, M. Shalom, L. Grinis, and A. Zaban, Phys. Chem. Chem. Phys. **15**, 3841 (2013).
[2] M. Mehrabian and R. Masoomi, J. Nanoelectr. Optoelectr. **10**, 633 (2015).
[3] A. Janotti and C. G. Walle, Rep. Prog. Phys. **72**, 126501 (2009).
[4] M. Mehrabian and S. Aslyousefzadeh, Adv. Sci. Eng. Med. **7**, 195 (2015).
[5] W. Lee, J. Lee, S. K. Min, T. Park, W. Yi, et al., Mater. Sci. Eng. **B156**, 1 (2009).
[6] D. C. Lim, W. H. Shim, K. D. Kim, H. O. Seo, J. H. Lim, et al., J. Solar Energy Mater. Solar Cell. **95**, 11 (2011).
[7] J. H. Borja, Y. V. Vorobiev, and R. R. Bon, J. Solar Energy Mater. Solar Cell. **95**, 7 (2011).
[8] H. M. Garcia, M. T. S. Nair, and P. K. Nair, Thin Solid Films **519**, 21 (2011).
[9] S. H. Im, H. J. Kim, and S. I. Seok, Nanotechnology **22**, 395502 (2011).
[10] M. F. Malek, M. Z. Sahdan, M. H. Mamat, M. Z. Musa, Z. Khusaimi, et al., Appl. Surf. Sci. **275**, 75 (2013).
[11] M. Mehrabian, H. Afarideh, K. Mirabbaszadeh, L. Lianshan, and T. Zhiyong, J. Opt. Soc. Korea **18**, 4 (2014).
[12] Z. Yang, Q. Zhang, J. Xi, K. Park, X. Xu, et al., Sci. Adv. Mater. **4**, 10 (2012).